Five-year results of a slant-path propagation experiment at 20 GHz in Madrid

J. M. García-Rubia
Universidad de Jaén, Linares, 23700, Spain

J. M. Riera, P. García-del-Pino, A. Benarroch
Universidad Politécnica de Madrid, Madrid, 28040, Spain

I. Introduction

Satellite operators are starting to use the Ka-band (30/20 GHz) for communications systems requiring higher traffic capacity. The use of this band is expected to experience a significant growth in the next few years, as several operators have reported plans to launch new satellites with Ka-band capacity. It is worth mentioning the Ka-Sat satellite in Europe, launched in 2010, and ViaSat-1, of 2011, with coverage of USA[1]. Some other examples can be found in other parts of the World. Recent satellite communications standards, such as DVB-S2[2] or DVB-RCS[3], which provide means to mitigate propagation impairments, have been developed with the objective of improving the use of the Ka-band, in comparison with previous technical standards. In the next years, the ALPHASAT satellite will bring about new opportunities[4] for carrying out propagation and telecommunication experiments in the Ka- and Q/V-bands.

Commercial uses are focused on the provision of high speed data communications, for Internet access and other applications. In the near future, it is expected that higher and higher data rates will also be needed to broadcast richer multimedia contents, including HD-TV, interactive content or 3D-TV. All of these services may be provided in the future by satellites of the current generation, whose life span can extend up to 2025 in some cases.

Depending on local regulations, the available bandwidth for the satellite fixed and broadcasting services in the Ka-band is in excess of several hundred MHz, bidirectional, comprising more than 1 GHz for each sub-band in some cases.

In this paper, the results of a propagation experiment that is being carried out at Universidad Politécnica de Madrid (UPM), Spain, are presented[5]. The objective of the experiment is twofold: gathering experimental time series of attenuation and analyzing them in order to characterize the propagation channel at these frequencies[6]. The experiment and statistical results correspond to five complete years of measurements.

The experiment is described in more detail in Section II. Yearly characteristics of rain attenuation are presented in Section III, whereas Section IV is dedicated to the monthly, seasonal, and hourly characteristics. Section V covers the dynamic characteristics of this propagation effect, just before the conclusions are described in Section VI.

II. Experimental setup

The experiment uses a satellite receiver, designed and built at the University, which measures the Eutelsat HB-6 Ka-band beacon at 19.7 GHz, and a radiometer working in the same frequency band[7]. The beacon receiver is able to measure rain attenuation and tropospheric scintillation, with a sampling rate of 18.66 Hz. The radiometer is used to measure gas and cloud attenuation, and to determine the 0-dB attenuation level.

Propagation results can be related to meteorological data obtained from several instruments co-located with the satellite receiver. An automatic meteorological station is available at the University premises, including sensors for pressure, temperature, humidity, wind and rain. A tipping-bucket rain gauge allows the measurement of rain intensity with 1-min integration time. Also, a Doppler radar (Micro Rain Radar) and an optical disdrometer have been installed, allowing also the measurement of rain profiles[8], including drop size distribution and rain intensity at different heights.

According to the measurements, the satellite beacon EIRP (Equivalent Isotropic Radiated Power) is probably around 17 dBW, well in excess of the 9 dBW specified by the satellite operator. The link elevation is 40.2°. Madrid is located at a height of 630 m. above sea level. It is situated in the center of the Iberian Peninsula, with continental climate. Rain occurs mainly in spring and autumn, being the average rainfall about 440 mm per year.

The receiver antenna is based on a centered Cassegrain structure, with an estimated gain of 45 dBi (1.2 m diameter).

The experiment has been running continuously for more than five years now. The results presented in this paper correspond to five complete years, from July 2006 to June 2011. The propagation measurements availability goes from 98.8% in the fifth year to 100% in the fourth year, with regards to rain attenuation. The remaining time include outage intervals that were concurrent with the presence of rain. The raingauge was available at 100% of the time. Rain events that occured during outage intervals of the propagation measurements system have been eliminated from the time series of rain intensity.
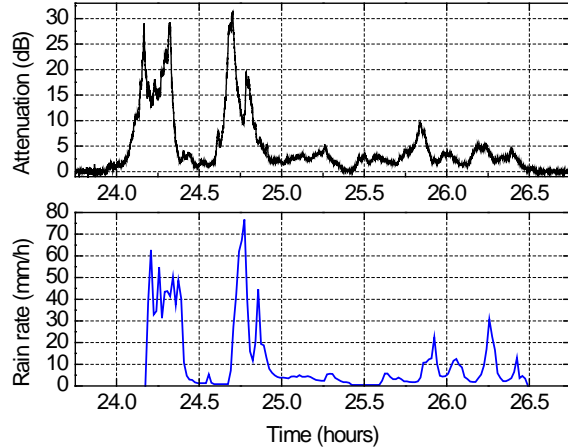
III.   Rain attenuation

Rain attenuation is the main propagation impairment in this band. The time series of rain rate, with 1- minute integration time, are used to identify the presence of rain and the approximate duration of the events. However, the raingauge measurements are insufficient, as rain rate is only measured at the receiver site, whereas rain attenuation may be due to rain at any point of the path. Moreover, the temporal resolution is different, as propagation measurements have a sampling rate of 18.66 Hz.

The start and end of each individual rain event is manually determined from the concurrent observation of the time series of attenuation and rain rate. The reference 0-dB attenuation level is interpolated from reference points, usually taken before and after the event.
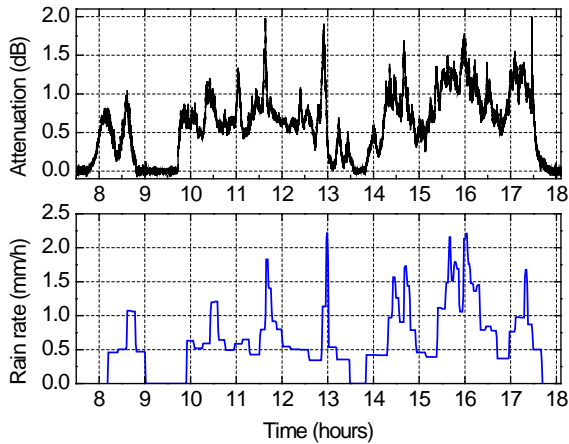
Figure 1. Stratiform rain event on 12th of January in 2010

Figure 2. Convective rain event on 11th of October in 2008

An example of long duration (10 hours) stratiform rain event, with low rainfall rate and attenuation, is displayed in Fig. 1. The time correlation between both series is remarkable, with peaks and lows almost coincident in time. This behavior is characteristic of this kind of precipitation that probably affects the whole path of the signal in the rain zone of the troposphere.

Figure 2 shows an example of a high intensity rain event of short duration; a peak of 77 mm/h (1-min integration time) is registered while the signal is attenuated about 30 dB from the reference level. The time series of attenuation and rain intensity follow similar trends, though some divergences arise for the highest values. It must be taken into account that the signal level is affected by rain present along the path within the rain zone of the troposphere, while rain intensity is measured only at the site location.
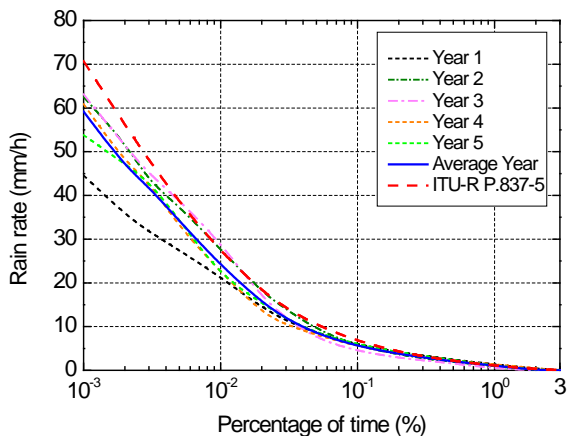
Figure 3. Cumulative distributions of rainfall rate
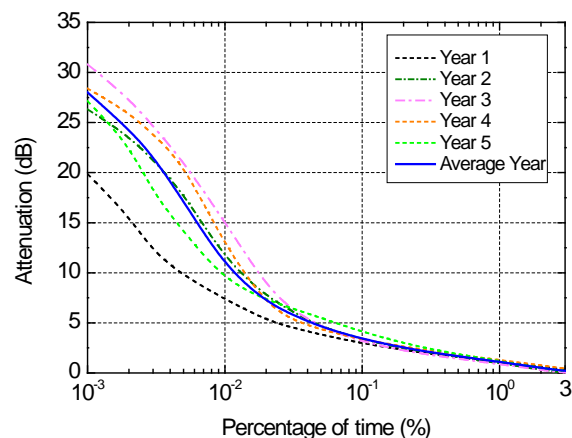
Figure 4. Cumulative distributions of rain attenuation

In Fig. 3, the rainfall rate distributions calculated from the rain gauge data are shown, using one-minute integration time, for the five years of measurements. Year 1 includes the twelve consecutive months from July 2006 to June 2007, whereas year 2 comprises from July 2007 to June 2008, and so on, until year 5 from July 2010 to June 2011. The

distribution for the average year is also shown. The experimental distributions are compared with the one derived from the ITU-R Rec. 837-5 rain intensity maps[9].

The rainfall rate exceeded for 0.01% of the average year, $R_{0.01}$, deserves special attention as it is used in the ITU-R model of rain attenuation[11]. The experimental values of $R_{0.01}$ reaches the maximum of 28.2 mm/h for the year 3, and the minimum at 21.3 mm/h for the year 1, and 24 mm/h for the average year. These values are not far from that predicted by the ITU-R Rec. P.837-5, 27.1 mm/h.

The cumulative distributions of rain attenuation in the five years of the experiment are shown in Fig. 4, as well as the distribution for the average year. The results are very similar for time percentages greater than 0.1%. However, significant differences appear in the 0.001-0.1% range, which is possibly the most important, as most communication and broadcast systems require availability in excess of 99.9%. For example, the attenuation exceeded 0.01% of the first year is in the order of 7 dB, whereas it is higher than 15 dB in the year 3. Similarly, the attenuation level exceeded 0.001% of the time is between 20 dB and 30.8 dB in the first year and third year, respectively. Thus, yearly variability can exceed 28% for such time percentages. The attenuation in the average year exceeded 3.4 dB for 0.1% of the total time, 10.6 dB for 0.01% and 28 dB for 0.001%.

The average year distribution has been compared with a large number of rain attenuation prediction models, which can be consulted in Ref. 10 or individually in Ref. 11-26. The measured distribution of the rain rate for the average year, presented in Fig. 3, has been used in most cases. The exceptions are the ITU-R model, that only needs $R_{0.01}$; the Crane Two-Component model, that includes its own rain distribution; and Synthetic Storm Technique that needs the rainfall rate time series for the five-year period.

Figures 5-7 show the predictions of the different rain attenuation models regarding the cumulative distribution of attenuation. These are compared with the average year experimental distribution. The errors between the measured and the predicted attenuation values have been calculated following the procedure described in ITU-R Rec. P.311-13[27].
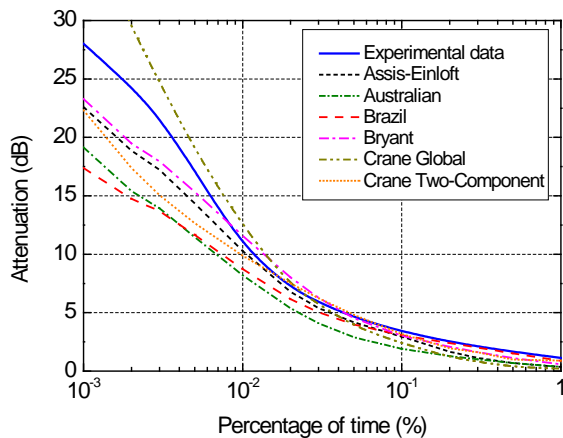
Figure 5. Comparision of experimental distribution with several rain attenuation models (I)
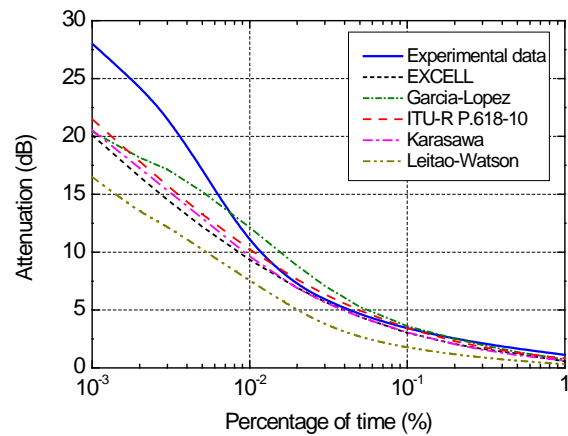
Figure 6. Comparision of experimental distribution with several rain attenuation models (II)
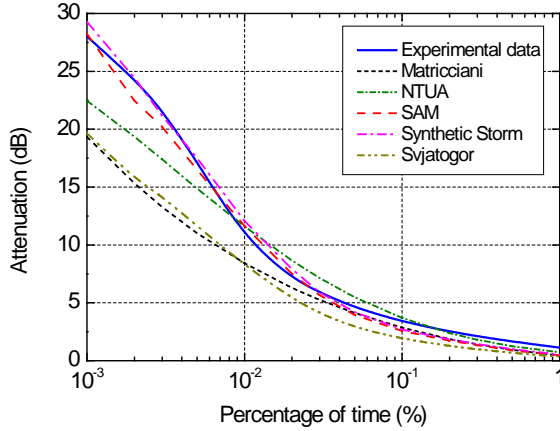
Figure 7. Comparision of experimental distribution with several rain attenuation models (III)

Model	RMS (%)
NTUA[23]	17.53
ITU-R P.618-10[11]	18.37
Garcia-Lopez[19]	18.73
Bryant[15]	19.42
Synthetic Storm[26]	20.52
Crane Two-Component[17]	22.02
Karasawa[20]	23.58
SAM[24]	24.69
EXCELL[18]	25.72
Brazil[14]	27.29
Assis-Einloft[12]	33.34
Matricciani[22]	34.75
Svjatogor[25]	46.48
Australian[13]	46.54
Crane Global[16]	52.74
Leitao-Watson[21]	55.37

Table 1. Rms errors between experimental and model predicted attenuation

Table 1 lists the rms errors between each model and the experimental data measured for the average year of the study period. Beginning the list, the models with lowest rms error are the NTUA, ITU-R, Garcia-Lopez, Bryant and Synthetic Storm Tecnique models all of them with errors up to 20.5%. At the end of the list, there are the highest rms error models, like Svjatogor, Australian, Crane global and Leitao-Watson.

IV.   Seasonal, Monthly and Hourly Variations of Attenuation

In broadcasting and data applications, the service availability in the average year may be complemented by more detailed measurements to better characterize the quality of service perceived by the final user.

Monthly variations are significant under the climatic conditions of Madrid. For example, the distributions of rain attenuation for the twelve months of the third year (July 2008-June 2009) of the experiment are shown in Fig. 8. For all time percentages, the minimum attenuation is in July, as only very light rain was registered during that month, reaching only 0.84 dB for 0.001% of the month. The maximum attenuation is around 1.8 dB for 1% of the month (October and December 2008), 7.5 dB for 0.1% of the month (October 2008) and 31 dB for 0.01% of the month (June 2009).

Traditionally, the worst month concept has been used to complement the information on the system performance throughout the year. The worst month of the third year, composed by the monthly distributions of September, October, December, June, is shown in Fig. 9.

Also Fig. 9 represents the average worst month attenuation distribution for the five years of the experiment, as well as the predicted one starting from the average year distribution of attenuation and converting it into worst month statistics using the procedure described in ITU-R Rec. P.841-4[28]. This procedure gives higher values in this case. The attenuation exceeds 14 dB for 0.005% of the worst month, higher than the 10.2 dB value measured for the average year.
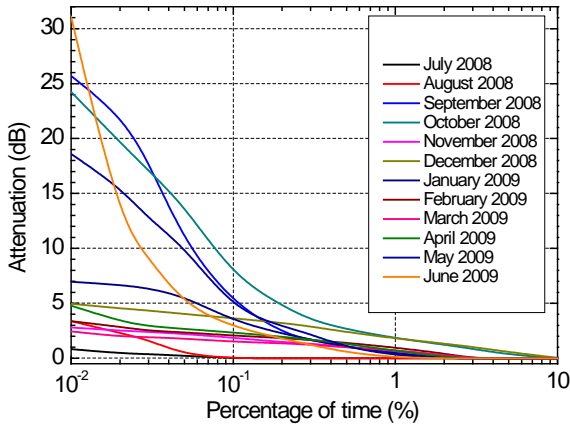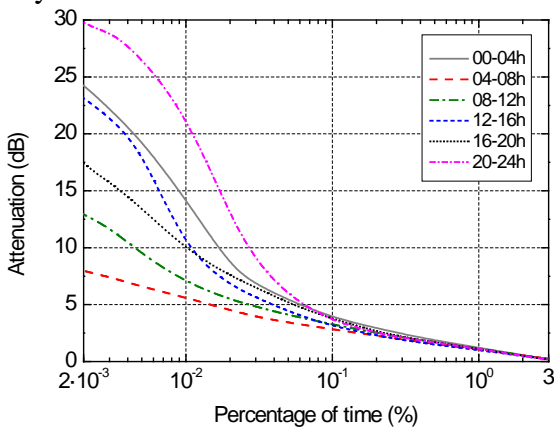
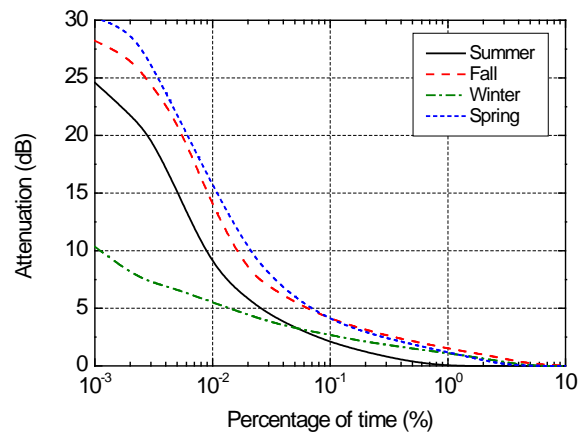**Figure 8. Monthly distributions of rain attenuation in year 3**
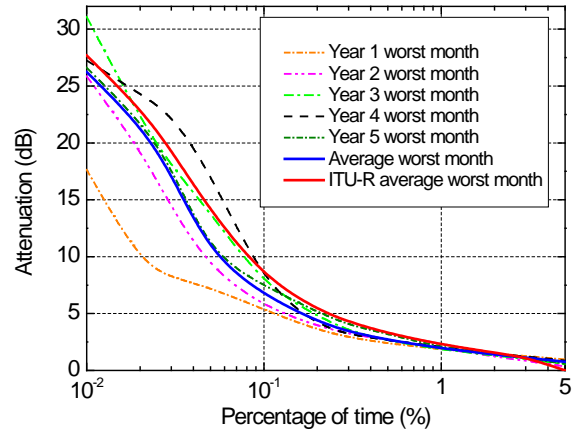
Figure 9. Distributions of rain attenuation for worst month

The hourly attenuation distributions are shown in Figure 10, for time intervals of 4 hours throughout the day. For the climatic conditions of Madrid, the highest intensity rain events occur in the afternoon (12-16h) and evening and first part of the night (20-4h), while they are less frequent at late night and in the morning (4-12h). It can be seen that 0.01% attenuation is around 21 dB in the evening time interval, compared with 5-7 dB in the morning intervals and 10.6 dB in the average year. There are no significant differences for the highest time percentages, above 0.1%.

In conclusion, broadcasting applications, in which a few evening hours concentrate the highest audiences, may suffer more from rain attenuation than professional data applications, whose need is more evenly distributed throughout the working hours of the day.

Figure 10. Distributions of rain attenuation for hourly intervals in the average

Figure 11. Distributions of rain attenuation for seasons in the average year

In Fig. 11 the seasonal attenuation distributions are illustrated for the average year of the five-year period of study. Again high differences in attenuation are shown among the time intervals of the average year, in this case for seasonal intervals. The rainy seasons are fall (from October to December) and spring (from April to June) especially. Winter (from January to March) has very lowest attenuation below 0.05% of time. Above that percentage of time, the summer (from July to September) has lower attenuation. It is interesting to note the important attenuation that can be reached in summer for low

percentages of time, 25.6 dB for 0.001%, due to a few convective rain events that produce high attenuation only during a few minutes.

Five years of data are perhaps a short period to obtain conclusive results regarding the average year cumulative distribution of attenuation. For this reason the experiment is being continued with the objective of gathering more than of six years' data.

Moreover, it is true that quantitative conclusions regarding monthly, hourly or seasonal distributions are less stable, as the five years of measurements are classified into twelve monthly intervals, six hourly intervals or seasonal intervals. So a qualitative conclusion can be pointed out with regards to rain attenuation: significant differences may be expected between different years, between different months, between different hourly intervals throughout the day, or between seasons in a year. This is also supported by climatic information regarding the irregular distributions of rain in Madrid.

V. Fade dynamics

The effects of fades on the quality of service perceived by the final user are very much conditioned by their duration. Although the cumulative distributions presented in Sections III and IV give important information, such as how much time in the year (or month, or in the worst month, or in a given hourly interval, or in a season) fades exceed a threshold of rain attenuation in dB, this information should be completed with parameters that allow the characterization of the fade dynamics.

In a broadcasting service, short fades that last for a few seconds, with pixels or frozen images in the TV screen, can be more tolerable than longer intervals of signal loss, even if they add to the same total time of fades in the year. In data applications, the lost data must usually be retransmitted. In some cases, longer fades can be more bearable than a multitude of shorter ones.

On the other hand, modern communication systems include some kind of link adaptation, or fade mitigation technique, that can be tuned to the expected durations of fade, or interfade, intervals.

The parameters used to characterize the fade dynamics in this paper have been taken from ITU-R Rec. P. 1623-1[29], and are considered to be the standard in this field. Two distribution functions are considered:

1. $P(d > D \,|\, a > A)$, the probability of occurrence of fades of duration d longer than D (s), given that the attenuation a is greater than A (dB). This probability can be estimated from the ratio of $N(d > D \,|\, a > A)$, the number of fades of duration longer than D, to the total number of fades observed, given that the threshold A is exceeded, $N_{tot}(A)$.

2. $F(d > D \,|\, a > A)$, the cumulative exceedance probability, or, equivalently, the total fraction (between 0 and 100%) of fade time due to fades of duration d longer than D (s), given that the attenuation a is greater than A (dB). This probability can be estimated from the ratio of the total fading time $T(d > D \,|\, a > A)$, due to fades of duration longer

than D given that the threshold A is exceeded, to the total exceedance time of the threshold, $T_{tot}(A)$. This can be obtained from the cumulative distribution of attenuation.

Similar parameters can be calculated for the interfade intervals, just by changing the condition $a > A$ into the complementary one $a < A$.

For this study, rain attenuation has been decimated to 1 Hz; as a consequence, the minimum fade duration is 1 second.

In Fig. 12, the total number of fades for the average year of the experiment is represented, for fade thresholds of 3, 5, 10 and 15 dB, and plotted versus the fade durations. It can be seen that there were around 1200 fades of more than 3 dB in the average year of the experiment, but only 22.8 were of more than 15 dB. Only 283.6 fades of more than 3 dB and 10.6 fades of more than 15 dB lasted for more than 10 seconds. Of these, 73.8 3-dB fades and 4.6 15-dB fades had durations in excess of 120 seconds, long enough to cause significant service disruptions in some commercial systems.
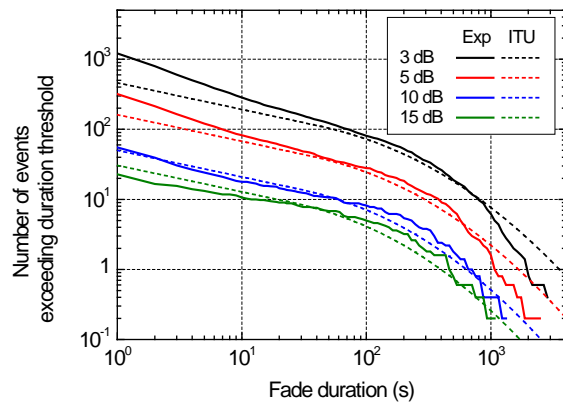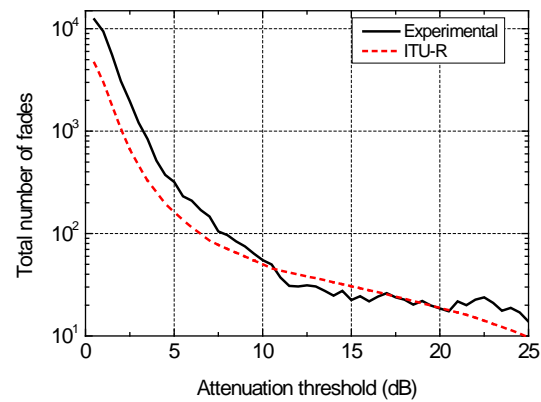

Figure 12. Number of fades

**Figure 13. Total number of fades**

The ITU-R Rec. P. 1623-1 includes a prediction model of fade dynamics in slant path propagation. The results of this model are also shown in Fig. 12. The comparison of the experimental and predicted curves is satisfactory, considering that the number of events is usually small for high attenuation thresholds like 15 dB. The ITU-R model provides lower values for most fade durations.

In Fig. 13 the total number of fades versus attenuation threshold are shown. It is remarkable the behavior of ITU-R model between 10 and 20 dB, clearly underestimating the total number of events below the threshold of 10 dB. The ITU-R estimation depends on total time for each threshold $T_{tot}(A)$. And $T_{tot}(A)$ has been determined empirically, from the local data, so the experimental fit is much better. If long-time statistics are not available, they can be estimated, using ITU-R Rec. P.618-10[11].

The probability of occurrence is obtained by normalizing the curves in Fig. 12 to the total number of fades for each attenuation level. The results are shown in Fig. 14. It is not unexpected that these curves are quite similar for the different attenuation levels. The 15-dB curve is more irregular, though this may be the result of the reduced number of events (only 22.8 per year) for this attenuation. The ITU-R model predictions are good for the

higher attenuation thresholds, getting an rms error of 22% for 10 dB, and 49% for 15 dB. The CRC model prediction[30] is good for low thresholds, reaching a 38% for 5-dB threshold. The overall rms error is 88% for ITU-R model and 64% for CRC model, although it is difficult to obtain a final conclusion about which one has better behaviour.
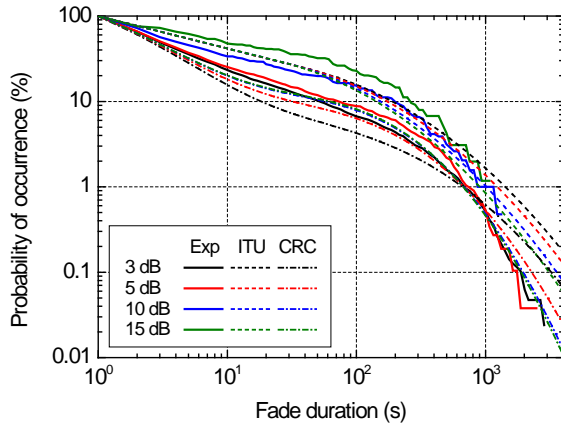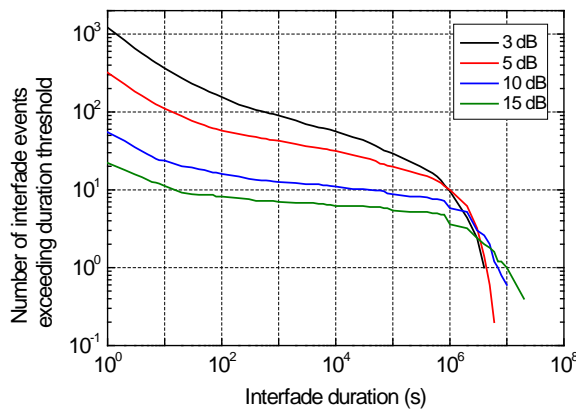

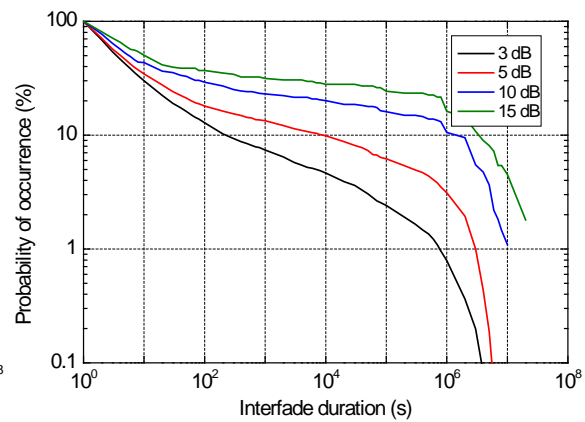**Figure 14. Probability of occurrence**
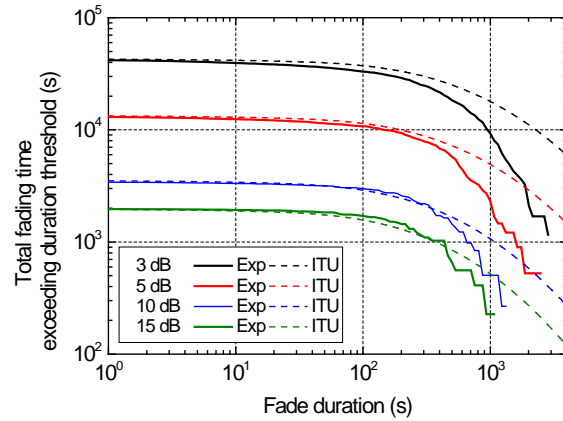
Figure 15. Total fading time

The distribution of the total time of fades among the different possible fade durations is shown in Fig. 15. For example, 5-dB fades comprise 221.35 minutes in the average year. Almost all this time comes in fades that last more than 10 seconds, causing system unavailability events if the margin is exceeded. The total time of 5-dB fades whose duration exceeded 120 seconds is about 184 minutes. The curves go down quickly in the interval of 100-1000 seconds.

Here the ITU-R model fit is tight for all the attenuation thresholds until 100-second durations; for durations above 100 s, the fall is modelled by a log-normal distribution. The total fades time distribution finds application in the design of fade mitigation techniques, as the expected durations of fades can be used in the design of the link control systems. Other applications are related to the characterization of the quality of service.

Figure 16. Number of inter-fade events

Figure 17. Probability of occurrence for inter-fade events

In Figure 16, the total numbers of interfade events are plotted versus their durations. The numbers of events slowly drop as their durations increase up to 10^6 seconds (11.6 days). Then, the slopes get steeper. The longest registered durations of the intervals between fades have been of 55 days for 3 dB, 73 days for 5 dB, 203 days for 10 dB and 243 days for 15 dB. As for the rest of measurements, rain events coincident with periods of receiver unavailability have not been considered. For these statistics, this procedure could cause a small change in the curves that would only affect the longest interfade durations.

When the curves in Fig. 16 are normalized to the total number of interfade events, the results shown in Fig. 17 are obtained. Significant differences appear between the curves. Thus, the probability of occurrence depends on the attenuation level. This is not the case previously shown in Fig. 14 for the fade durations. To our knowledge, there is no available prediction model for interfade durations. Through the comparison of Fig. 14 and 17, it can be concluded that similarities exist in the behaviour of fade and interfade duration distributions. However, there are also significant differences in the time scales and in the dependence on the attenuation level shown in Fig. 17.

Fade slope statistics have also been calculated. Following standard practices, the attenuation time series are low-pass filtered before computing fade slopes, in order to eliminate scintillation and to remain the slopes due to rain attenuation and other slow effects like clouds. Depending on the filtering quality of fast components, the slopes obtained could be different. In this case, a 5th-order Butterworth low-pass filter with 0.02 Hz cut-off frequency has been used. This 3-dB cutoff frequency is recommended in the ITU-R Rec. P.1623-1. The definition of fade slope ζ is shown in Eq. 1.

$$\zeta(t) = \frac{A\left(t + \frac{1}{2}\Delta t\right) - A\left(t - \frac{1}{2}\Delta t\right)}{\Delta t} \quad \text{dB/s} \tag{1}$$

The fade slope ζ is associated to the attenuation $A(t)$ that takes place in the middle point of the time interval of Δt seconds.

Fade slope distributions are shown in Fig. 18 and 19. These figures give basically the same information, Fig. 18 is the probability density function and Fig. 19 the cumulative distribution function. The fade slopes are limited to the attenuation thresholds of 3, 5, 10, 15 and 20 dB (the attenuation levels in the ITU-R Rec. P.1623 are from 0 to 20 dB) and the time interval is 30 seconds (ITU-R Rec. P.1623 uses time intervals between 2 and 200 seconds). ITU-R model predictions are also shown for comparison.

Statistics are remarkably close to the predictions from the ITU-R model, though differences are higher for the lower probabilities and for the highest attenuation thresholds. Both cases present smaller amounts of experimental data. To compare ITU-R model and experimental data, the rms error has been calculated by ITU-R Rec. P.311-13.

For the case of accumulated distribution in Fig. 19, the fit is very tight for the 3-dB attenuation, with a very low rms error of 3.82%. When the attenuation increases the fit

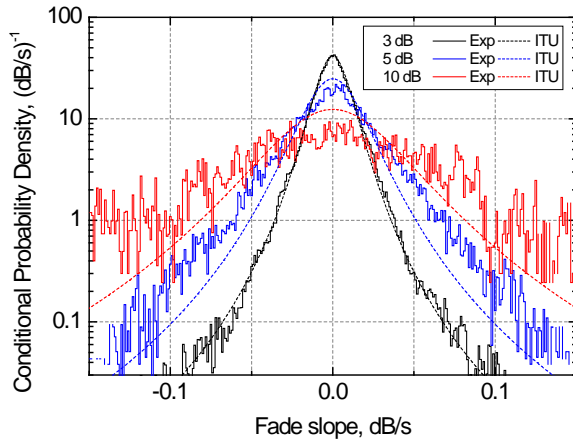loses precision, so the 5-dB rms error is 31.11%; at 10-dB, 50.47%; at 15-dB, 60.45%, and at 20-dB, 52.23%.

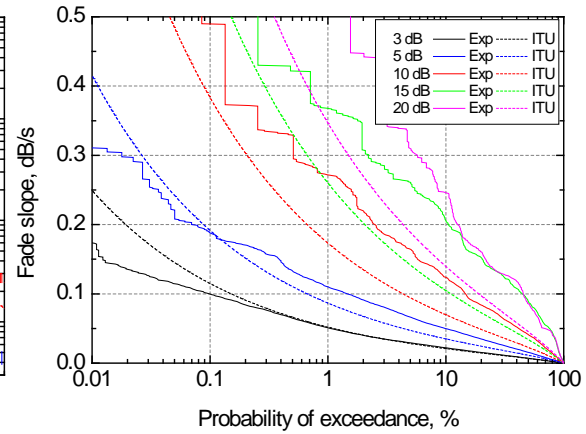**Figure 18. Probability distribution of fade slope**

Figure 19. Cumulative distribution of fade slope

VI.   Conclusion

A propagation experiment is being carried out in Madrid, Spain, with the objective of characterizing the effects that affect the Ka-band signal in the slant-path. The results show that, as expected, propagation effects in this band are more relevant than at lower frequencies, with rain attenuation exceeding 10.6 dB for 0.01% of the year. Moreover, attenuation presents a wide variability. It can be significantly higher for the same time percentage for a particular year, such as the third year of the experiment, for a particular month, or for a particular time interval within the day. For example, it has been shown that attenuation is above 10 dB for 0.01% of the time if only the afternoon and evening hours are considered. These include the prime time TV audience, and should be considered in the design of broadcasting systems. Unfortunately, available propagation models only consider the average year and worst-month statistics, and do not take into account year-to-year, seasonal or hourly variability.

The research includes the dynamic characteristics of attenuation, in particular the duration of fade, interfade events and fade slope, as this information is of interest for the design and simulation of the performance of systems that incorporate fade mitigation techniques, such as power control or adaptive modulation and coding. The experimental results have been compared with ITU-R prediction models, showing the good fit for an important range of probability and attenuation thresholds.

Propagation impairments are important in this band, but techniques exist that can be of help to mitigate their effects. These techniques include several variants of link adaptation (power control, adaptive modulation and coding, rate reduction) as well as site, satellite or frequency band diversity. The huge amounts of available bandwidth, as well as technical advantages, such as the use of smaller antennas, are strong arguments in favor of its use, even with reduced service availability in some cases.

References

[1] D. Freyer, "Ka-Band: Ready to make a business impact?", Via Satellite Magazine, XXIII, 9, September 2008, pp. 26-32.

[2] DVB-S2 ETSI EN 302 307 v1.1.2, Digital Video Broadcasting (DVB); Second generation framing structure, channel coding and modulation systems and modulation systems for Broadcasting, Interactive Services, News Gathering and other broadband satellite applications, Sophia Antipolis, France, ETSI, 2006.

[3] DVB-RCS ETSI EN 301 790 v 1.5.1, Digital Video Broadcasting (DVB); Interaction channel for satellite distribution systems, Sophia Antipolis, France, ETSI, 2009.

[4] A. Paraboni et al, "Description of Alphasat TDP5 Experiment", ESA Workshop on Radiowave Propagation Models, Tools and Data for Space Systems, ESTEC, Noordwijk, The Netherlands, December 2008.

[5] J.M. Riera, A. Benarroch, P. García, J.M. García, "Radiowave Propagation Experiments in Madrid", ESA Workshop Radiowave Propagation Models, Tools and Data for Space Systems, 3-5 Dec. 2008, ESTEC, Noordwijk, The Netherlands.

[6] Garcia-Rubia, J.M.; Riera, J.M.; Garcia-del-Pino, P.; Benarroch, A., "Propagation in the Ka Band: Experimental Characterization for Satellite Applications," Antennas and Propagation Magazine, IEEE , vol.53, no.2, pp.65-76, April 2011

[7] P. García, J. M. García, J. M. Riera, and A. Benarroch, "Slant-path propagation experiment at Ka-band in Madrid", *Proc. of EuCAP,* Edimburgh, UK, 12-16 November 2007.

[8] P. Garcia-Vila, A. Benarroch, P. Garcia, and J.M. Riera, "Micro Rain Radar measurements of rainfall in Madrid," Proc. of 3rd European Conference on Antennas and Propagation (EuCAP), Berlin, Germany, 23-27 March 2009, pp.676-680.

[9] ITU-R, "Characteristics of precipitation for propagation modelling", Recommendation ITU-R P.837-5, ITU Radiocommunication Bureau, Geneva, Switzerland, 2007.

[10] COST Action 255 Final Report: Radiowave Propagation Modelling for SatCom Services at Ku-Band and Above, ESA Publications Division, ESTEC, Noordwijk, the Netherlands, 2002.

[11] ITU-R, "Propagation Data and Prediction Methods Required for the Design of Earth-Space Telecommunication Systems", Recommendation ITU-R P.618-10, ITU Radiocommunication Bureau, Geneva, Switzerland, 2009.

[12] M. S. Assis and C. M. Einloft, "A simple method for estimating rain attenuation distribution", Annals of Telecommunications, vol. 32, (11), pp. 478-480, 1977.

[13] R. K. Flavin, "Satellite link rain attenuation in Brisbane and a proposed new model for Australia", Telstra Research Laboratories, Report N. 8375, 1996.

[14] CCIR Document 5C/52 (Brazil), "Slant-path Attenuation Prediction Method Based on the Complete Point Rainfall Rate Distribution", ITU, Geneva, Switzerland, 1992.

[15] G. H. Bryant, I. Adimula, C. Riva and G. Brussaard, "Rain attenuation statistics from rain cell diameters and heights", Int. J. Satellite Commun., vol. 19, (3), pp. 263-283, 2001.

[16] R. Crane, "Prediction of attenuation by rain", IEEE Trans. Commun., vol. 28, (9), pp. 1717-1733, 1980.

[17] R. K. Crane, "A two-component rain model for the prediction of attenuation statistics", Radio Sci., vol. 17, pp. 1371-1387, 1982.

[18] C. Capsoni, C. Magistroni, A. Paraboni, A. Pawlina and F. Fedi, "Data and theory for a new model of the horizontal structure of rain cells for propagation applications", Radio Sci., vol. 22, (3), pp. 395-404, 1987.

[19] J. A. Garcia-Lopez, J. M. Hernando and J. M. Selga, "Simple rain attenuation prediction method for satellite radio links", IEEE Transactions on Antennas and Propagation, vol. 36, pp. 444-448, 1988.

[20] M. Yamada, Y. Karasawa, M. Yasunaga and B. Arbesser-Rastburg, "An improved prediction method for rain attenuation in satellite communications operating at 10-20 GHz", Radio Sci., vol. 22, pp. 1053-1062, 1987.

[21] M. J. Leitao and P. A. Watson, "Method for prediction of attenuation on earth-space links based on radar measurements of the physical structure of rainfall", in IEE Proceedings F Communications, Radar and Signal Processing, vol. 133, pp. 429-440.

[22] E. Matricciani, "Rain attenuation predicted with a two-layer rain model", Eur. Trans. Telecommun., vol. 2, (6), pp. 715-727, 1991.

[23] A. D. Panagopoulos, P. D. M. Arapoglou, J. D. Kanellopoulos and P. G. Cottis, "Long-term rain attenuation probability and site diversity gain prediction formulas", IEEE Transactions on Antennas and Propagation, vol. 53, (7), pp. 2307-2313, 2005.

[24] W. L. Stutzman and K. M. Yon, "A simple rain attenuation model for earth-space radio links operating at 10-35 GHz", Radio Sci., vol. 21, pp. 65-72, 1986.

[25]L. Svjatogor, "Prostranstvennaia korelacia vypadenjija dozdjej vdol zemnoj poverchnostji", Interkosmos Symposium, Theme 5 of the Established Telecommunication Working Group, 1985.

[26]E. Matricciani, "Physical-mathematical model of the dynamics of rain attenuation based on rain rate time series and a two-layer vertical structure of precipitation", Radio Sci., vol. 31, (2), pp. 281-295, 1996.

[27]ITU-R, "Acquisition, presentation and analysis of data in studies of tropospheric propagation", Recommendation ITU-R P.311-13, ITU Radiocommunication Bureau, Geneva, Switzerland, 2009.

[28]ITU-R, "Conversion of annual statistics to worst-month statistics", Recommendation ITU-R P.841-4, ITU Radiocommunication Bureau, Geneva, Switzerland, 2005.

[29]ITU-R Rec. P.1623-1, "Prediction method of fade dynamics on Earth-space paths", ITU, Genève, Switzerland, 2005.

[30]M. Cheffena and C. Amaya, "Prediction Model of Fade Duration Statistics for Satellite Links Between 10-50 GHz", IEEE Antennas and Wireless Propagation Letters, vol. 7, pp. 260-263, 2008.